Available online at www.sciencedirect.com

ScienceDirect

journal homepage: www.elsevier.com/locate/he

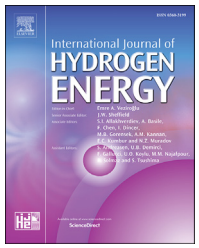

Short Communication

Mechanical activation of TiFe for hydrogen storage by cold rolling under inert atmosphere



L.E.R. Vega [a], D.R. Leiva [b,*], R.M. Leal Neto [c], W.B. Silva [a], R.A. Silva [b], T.T. Ishikawa [b], C.S. Kiminami [b], W.J. Botta [b]

[a] Programa de Pós-Graduação em Ciência e Engenharia de Materiais, Universidade Federal de São Carlos - UFSCar, Rod. Washington Luis, Km 235, CEP 13565-905, São Carlos, SP, Brazil

[b] Departamento de Engenharia de Materiais, Universidade Federal de São Carlos - UFSCar, Rod. Washington Luis, Km 235, CEP 13565-905, São Carlos, SP, Brazil

[c] Centro de Ciência e Tecnologia de Materiais, Instituto de Pesquisas Energéticas e Nucleares - IPEN, Av. Lineu Prestes, 2242 Cidade Universitária, CEP 05508-000, São Paulo, SP, Brazil

ARTICLE INFO

Article history:
Received 1 September 2017
Received in revised form
12 October 2017
Accepted 10 December 2017
Available online 4 January 2018

Keywords:
Cold rolling under inert atmosphere
Hydrogen storage
TiFe

ABSTRACT

TiFe is a very interesting material for hydrogen storage in the solid state, due to its hydrogen capacity of 1.9 wt % and to the fact it can be absorb/desorb hydrogen at room temperature. However, the TiFe produced by casting does not absorb hydrogen, unless a procedure called activation is applied, which is based on a repetition of several thermal cycles. This study evaluates the effects of a mechanical activation route for the TiFe intermetallic compound, namely, cold rolling (CR) under inert atmosphere. Stoichiometric TiFe was prepared from elementary powders by arc melting. Ingot was grinded and then cold rolled for 20 and 40 passes under argon inside a glove box, with moisture and oxygen contents below 0.1 ppm. Cold rolled samples consisted of two parts: powder particles and thin cracked flakes. The results showed that mechanically activated samples by CR exhibited rapid absorption of hydrogen at room temperature, without using a thermal activation process. In general, the average storage capacity of hydrogen was 1.4 wt% H_2 for the first absorption, regardless of the number of passes for both flake and powder samples.

© 2017 Hydrogen Energy Publications LLC. Published by Elsevier Ltd. All rights reserved.

Introduction

The development or adaptation of more effective processing techniques is an important research question, in order to allow the applications of the hydrogen storage materials [1,2]. TiFe is an attractive AB intermetallic compound of practical interest for hydrogen storage due to its hydrogen capacity (theoretically 1.9 wt %) at room temperature, along with the low cost of the constituent elements [3–6]. In spite of forming two hydride phases (TiFeH and $TiFeH_2$), bulk TiFe (prepared by casting) needs to be thermally activated in order to begin to absorb hydrogen [7]. To avoid this step, different authors have used different processing routes, such as: Mechanical Alloying (MA) from elementary powders aiming to produce TiFe in

* *Corresponding author.*
E-mail address: daniel.leiva@ufscar.br (D.R. Leiva).

https://doi.org/10.1016/j.ijhydene.2017.12.054

0360-3199/© 2017 Hydrogen Energy Publications LLC. Published by Elsevier Ltd. All rights reserved.

short time and with high grain refinement [8–13], Mechanical Milling (MM) or Mechanical Grinding (MG) of TiFe processed by arc melting to decrease particle size and increase surface area [8,11,14]. However, a thermal activation process is still required which can be related with oxidation that may occur during or after High Energy Ball Milling (HEBM), reducing the reactivity of TiFe with hydrogen [8].

In search of processing TiFe with low oxygen content and good ability to absorb hydrogen, techniques based on severe plastic deformation (SPD) such as high-pressure torsion (HPT), equal channel angular pressing (ECAP) and cold rolling (CR), could be an alternative. These techniques can produce materials with nanocrystalline structures, with increased defects density, as dislocations and grain boundaries, thus facilitating the synthesis of metal hydrides [15].

Recent studies showed that TiFe compound with good hydrogen absorption capacity was produced by HPT and groove rolling (GR) in the presence of air. However, it was necessary to use a heat treatment to reactivate the as-deformed material [16,17]. Decreasing the oxygen intake during the SPD processes could be a solution to avoid thermal reactivation of TiFe before hydrogenation step, as we reported before for Mg [18] and MgH_2 [19].

Therefore, the main objective of this study was to process TiFe by arc melting followed by CR under inert atmosphere. With the application of this new route, the aim was to obtain nanostructured TiFe; similar to that obtained by HEBM, but in shorter periods, and simultaneously enhance hydrogen absorption in the TiFe without the need for a thermal activation process.

Materials and methods

Ti (−100 mesh, 99.4%, Alfa Aesar) and Fe (−20 mesh, 99%, Alfa Aesar) powders were weighted with the stoichiometric ratio 50:50 and mixed in a planetary mill (Fritsch Pulverisette 6) without balls at a rotation speed of 200 rpm for 10 min. Powders were handled inside a glove box (MBRAUN LAB Master 130) with purified argon, with H_2O and O_2 levels below 0.1 ppm. The mixture was then compacted up to 95 MPa in air with a hydraulic press using a cylindrical die with 16.2 mm diameter. After compaction, pellets were arc melted (Arc MelterD72379 Edmund Bühler GmbH) under inert atmosphere. The ingot produced was remelted eight times to promote a better homogeneity.

After characterization, the TiFe ingot was first ground in a home-made vertical rolling machine located inside the glove box. The ground fragments were submitted to 20 and 40 rolling passes at a fixed roll rotation frequency of 50 rpm. The rolls dimensions were 6.4 cm in diameter and 8 cm length with a narrow "minimum allowed" spacing between the rolling cylinders. The rolled material after each pass was collected directly below the mill and was placed again on top of it. The process was repeated until the desired amount of passes was achieved. Rolled material consisted of two distinct parts: powder particles and flakes fragments. These parts were separated from each other by sieving (mesh size of 0.177 mm), in order to investigate the morphological effects on the hydrogen storage properties.

The TiFe ingot and the cold rolled samples were examined through X-ray diffraction (XRD) analysis in a Siemens D 5005 diffractometer using Cu K_α radiation at 40 kV and 40 mA. The crystallite size was estimated through the Scherrer equation using the description presented by Lu and Lai [20]. Scanning electron microscopy (SEM) was carried out in a FEI Inspect S50 microscope, equipped with energy dispersive X-ray spectrometry (EDS). Metallographic sample of the TiFe ingot was prepared by conventional means. Etching was accomplished in a solution of 67% H_2O, 3% HF and 30% HNO_3 before SEM. Transmission electron microscopy (TEM) was conducted in a FEI TECNAI G^2 F20 HRTEM. The oxygen levels of samples were measured using a LECO ONH836 elemental analyzer. To minimize the air contamination of the samples during their transport from the glove box to the oxygen analyzer, the sample holder was hermetically closed under the inert atmosphere of the glove box. Hydrogen storage properties were measured at room temperature under initial hydrogen pressure of 2 MPa using a homemade Sievert's type apparatus.

Results and discussion

Fig. 1 shows XRD patterns from TiFe ingot, powder and flakes after CR passes under inert atmosphere. Peaks of oxide phases were not observed in the XRD patterns, even after 40 rolling passes. In addition, an oxygen content of 0.23 ± 0.02 wt% was measured in the sample submitted to 20 rolling passes. This level of contamination is lower than those reported for TiFe processed by high energy ball milling (0.95–1.4 wt %) [8,13], evidencing that the use of this processing route has succeeded in minimizing contamination with oxygen. In previous studies from our group [18,19], it was also reported that Mg or MgH_2 when cold rolled under inert atmosphere did not present oxide phases, even for high number of passes as e. g. 50.

XRD analysis of the cold rolled powder and flake samples showed that the estimated crystallite sizes (Table 1) decreased accordingly to the number of passes. The estimated crystallite sizes are in the nanoscale and are comparable to those

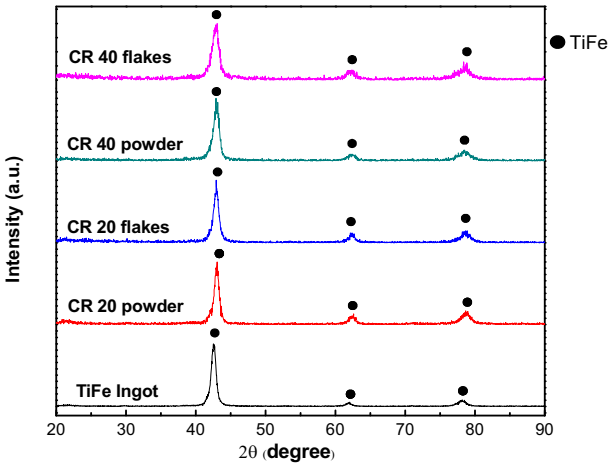

Fig. 1 – XRD patterns of the TiFe ingot (as-melted), cold rolled powder and flake samples after 20 (CR 20) and 40 (CR 40) passes.

Table 1 – Estimated crystallite sizes of TiFe submitted to CR under inert atmosphere.

Sample	CR20 powder	CR20 flakes	CR40 powder	CR40 flakes
TiFe crystallite size (nm)	11	11	9	7

reported in the literature for TiFe processed by high energy ball milling [8,9,13], which is a very interesting result considering the much shorter time and lower energy cost of the CR process when compared to HEBM. The nanostructure formation is known to considerably improve the hydrogen storage of the material [21]. A possible explanation for not having a significant change in crystallite size after 20 rolling passes is the attainment of a steady-state, in which there is a saturation of the decrease in the crystallite size [22]. This saturation was also reported in TiFe processed by HPT [16].

Fig. 2 shows SEM micrographs of the TiFe ingot, before and after rolling. As expected, it is observed that the as-cast microstructure is composed of coarse columnar grains (Fig. 2a) [16,17].

After 20 rolling passes, the sample consisted of small cracked flakes (Fig. 2b) and particles (Fig. 2c). After 40 passes, the amount of particles increased (Fig. 2d) in relation to the number of flakes. Fig. 2e shows the detail of the particles. In addition, flakes with higher number of cracks were observed (Fig. 2f) as the number of rolling passes increased. It is important to mention that the formation of particle agglomerates is common in the TiFe processed by HEBM [10,11,23] and in the cold rolled TiFe. On the other hand, crack

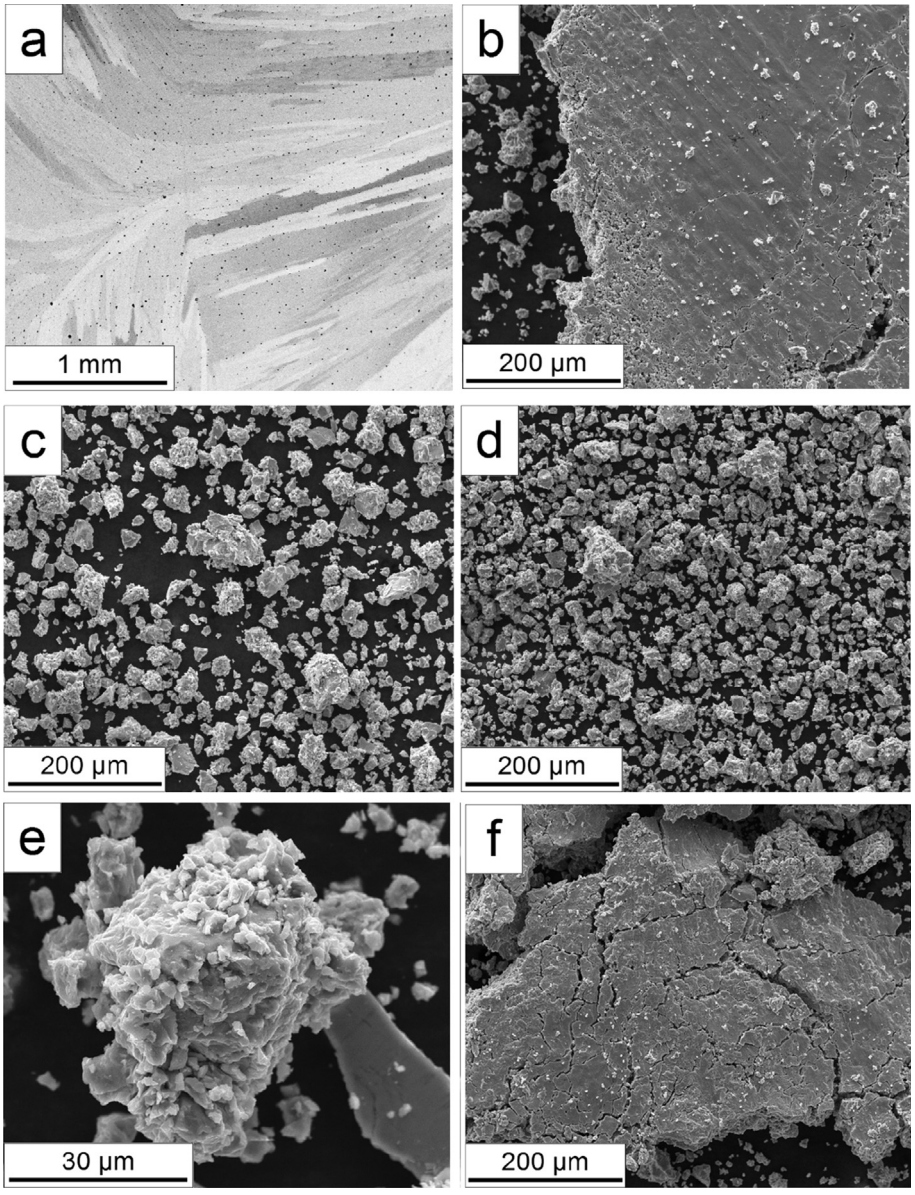

Fig. 2 – SEM micrographs of TiFe samples: melted ingot ((a) - backscattered electrons), and cold rolled material (secondary electrons), CR 20 (b, c), CR 40 (d, e, f).

formation was also observed in TiFe submitted to high pressure torsion and groove rolling, which can act as pathways for the transport of hydrogen from the surface to the interior of the samples [16,17]. Chemical composition of the ingot and cold rolled samples were evaluated by EDS. The average atomic percentage compositions of Ti and Fe elements are around 1:1, as expected (50.2 ± 0.12 at. % Ti and 49.8 ± 0.12 at.% Fe). It was shown for other systems, as is the case for Mg, that crystallographic texture can affect significantly the H-absorption behavior [24]. This effect cannot be easily analyzed for TiFe after CR, due to the shape and size of the samples, as seen on Fig. 2.

Fig. 3 shows TEM images of the cold rolled powder after 40 passes. The SAEDP (selected area electron diffraction pattern) shows only TiFe reflections, Fig. 3b, with ring format, which is typical for nanocrystalline materials. The dark-field image for the TiFe (110) planes, Fig. 3c, indicates that the sample has very low crystallite size, of around 10 nm, which is compatible with the crystallite size of 9 nm estimated by the analysis of XRD peaks. The TEM analysis confirms the ability of the CR process to refine the grain size of TiFe to a few nanometers, as shown before for Mg or MgH_2 [18,19]. The utilization of the combined techniques of XRD (Table 1) and TEM (Fig. 3) is an interesting strategy for the evaluation of the level of refinement of the microstructure [25]. However, the estimation of the crystallite size in each case may result slightly diverse, since the principles used in these methods are obviously different.

Fig. 4 shows kinetic curves for the first hydrogen absorption of the cold rolled samples, measured under initial 2 MPa of H2 at room temperature. Samples resulting from 20 and 40 rolling passes consisted of powder and flakes, which were separated, in attempt to better understand the effects of these distinct morphologies on the hydrogen storage properties.

No absorption of hydrogen was detected in the as-cast ingot of TiFe, in agreement with other reports [7,11,14,16,17,26]. On the other hand, after the mechanical activation provided by CR under inert atmosphere, samples reacted rapidly with hydrogen without the need of additional thermal activation process. CR20 and CR40 powder samples attained a maximum absorption capacity of 1.4 wt % H_2 after 4 h (Fig. 4a). Fig. 4b shows that CR20 and CR40 flakes samples had after 4 h a maximum absorption capacity of about 1.4 and 1.3 wt% H_2, respectively. CR40 powder and flakes samples exhibited faster kinetics at the beginning of hydrogen absorption, compared to the CR20 powder and flakes samples, which is possibly due to the increased surface area reached after more rolling passes [19]. However, at this point we cannot fully explain why the final capacity of the sample CR20 flake is a little bit higher than the CR40 flake, Fig. 4b. This can be due to structural or morphological reasons, as well as due to instrumental errors, since the difference is reasonably low (around 0.1% of hydrogen capacity).

It is important to mention that in the reports available to date, there is no information about studies on hydrogen storage properties of TiFe compound submitted to CR under inert atmosphere. However, there are studies on severe plastic deformation techniques HPT and GR applied to TiFe for hydrogen storage [16,17]. In these studies the research were focused on the PCI curves (equilibrium pressure x H_2 concentration measured isothermally) and not on the kinetic behavior.

Table 2 compares the reported hydrogen storage capacities from PCI curves with those found in the present study through kinetic curves. Different references mentioned in Table 2 reported the need of a heating process (423 K for 2 h under continuous vacuum) to make possible the hydrogenation of TiFe at room temperature. This need of activation could be

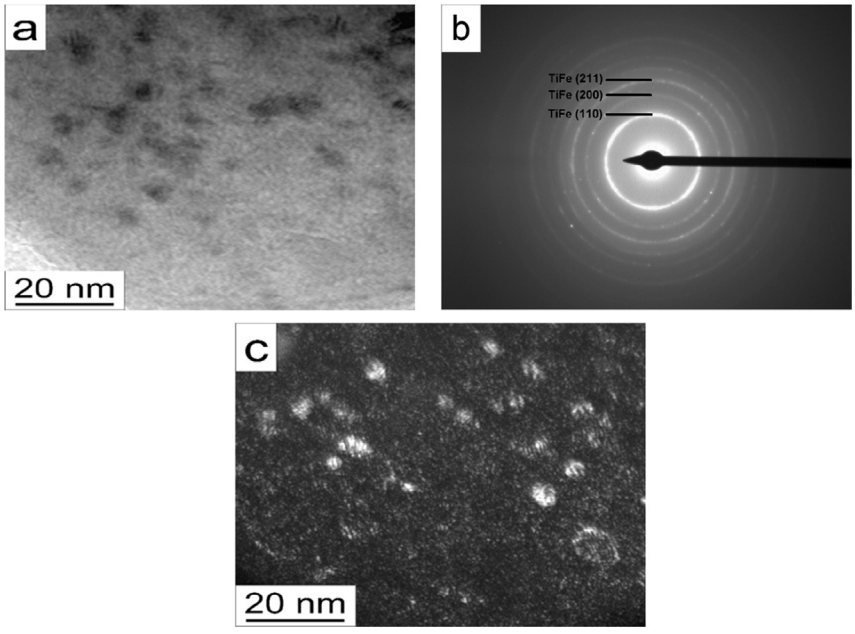

Fig. 3 – TEM of TiFe CR40 powder (a) bright-field image, (b) electron diffraction pattern, and (c) dark-field image obtained with reflections from the TiFe (110) planes.

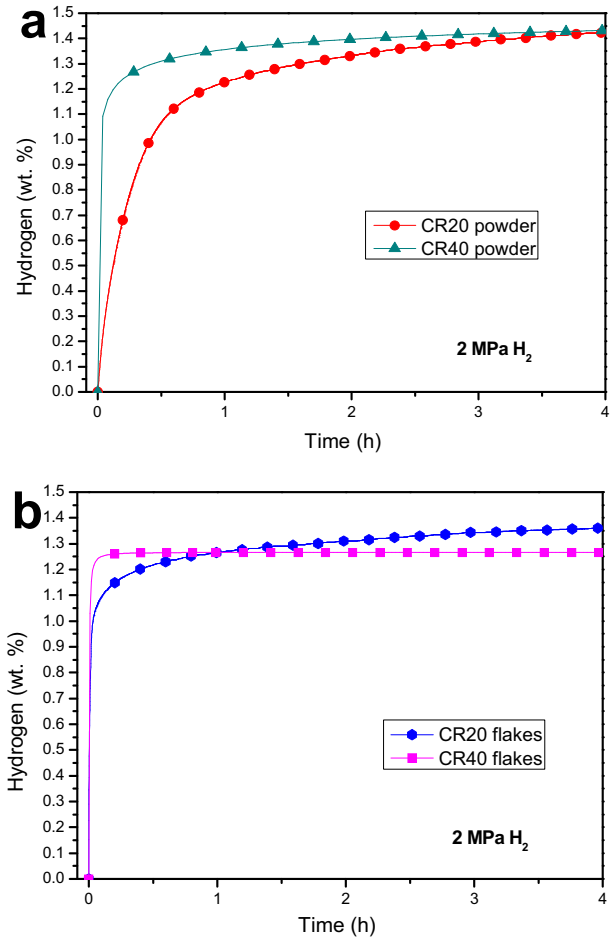

Fig. 4 – Kinetic curves of the first absorption of hydrogen (2 MPa) at room temperature of TiFe cold rolled samples: powder (a) and flake (b) after 20 and 40 passes under inert atmosphere.

associated to the formation of an oxide layer in the TiFe due to its processing in air [16,17]. In the present study, the adopted processing route allowed TiFe to react rapidly with hydrogen at room temperature, eliminating the need of a heat treatment step. The introduction of defects by cold rolling, which mechanically activated the melted TiFe, and the reduced oxygen contamination provided by the control of the working atmosphere provided good hydrogen absorption capacity, with the benefit of using a lower hydrogen pressure.

In an attempt to make a comparison of the hydrogen storage properties of the samples processed in this study with those presented in the literature for TiFe processed by HEBM,

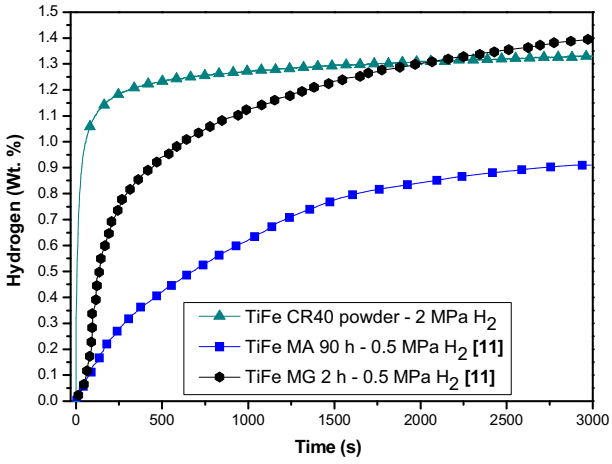

Fig. 5 – Kinetic curves of the first absorption of hydrogen at room temperature of the TiFe processed by HEBM [11] and of the TiFe CR40 powder sample (this study).

it was found that there is more information about PCI curves [8–10,12–14] than about kinetic curves [11]. So the kinetic curves reported for TiFe processed by HEBM was plotted with TiFe CR40 powder sample curve of this study in Fig. 5.

It is observed that the powder resulting from 40 passes of cold rolling under inert atmosphere (TiFe CR40 powder) showed a higher absorption capacity of hydrogen (~1.4 wt% H_2) after 3000 s, in comparison to TiFe processed by mechanical alloying in 90 h (TiFe MA 90 h, 0.9 wt % H_2). Moreover, the rolled sample presented approximately the same absorption capacity of hydrogen after 3000 s in relation to the TiFe processed by mechanical grinding in 2 h (TiFe MG 2 h). It is important to mention that the samples processed by Haraki et al. [11] required a heat treatment before the hydrogen absorption process (573 K for 2 h under continuous vacuum). This could be considered an activation process related to the oxidation phenomenon that can occur in HEBM [8]. In the case of this study, the use of a controlled atmosphere during CR provided enough protection against oxygen contamination and the activated state reached after deformation was sustained.

Another point evidenced by Fig. 5 is the significant difference in the hydrogen absorption capacity between the samples processed by CR under inert atmosphere and by mechanical alloying. This can be explained by different hydriding behaviors between TiFe processed by mechanical alloying (i.e. by HEBM of the elementary powders) and by mechanical grinding (i.e. milling of the TiFe intermetallic). It

Table 2 – Hydrogen absorption capacities obtained in this study compared to those observed in the literature.

Sample	Absorption conditions	Wt. % H_2	Reference
TiFe HPT	303 K, 8 MPa	1.7	[16]
TiFe GR	303 K, ~10 MPa	1.7	[17]
TiFe CR20 powder	Room temperature, 2 MPa	1.4	This study
TiFe CR20 flakes	Room temperature, 2 MPa	1.4	This study
TiFe CR40 powder	Room Temperature, 2 MPa	1.4	This study
TiFe CR40 flakes	Room Temperature, 2 MPa	1.3	This study

was reported that $TiFeH_2$ (γ phase) was difficult to be achieved by hydriding TiFe produced by mechanical alloying, due to highly-disordered amorphous regions present at the grain boundaries. This difficulty is reduced when TiFe is produced by mechanical grinding, since amorphous phase formation as well as lattice deformations are induced mainly in surface regions of a TiFe particle [11]. The results from the present work suggest that the effect of CR of the TiFe alloy is somewhat similar to the obtained for mechanical grinding.

Conclusions

TiFe processed through arc melting can be easily mechanically activated by CR under inert atmosphere after 20 or 40 passes. Hydrogen absorption rate is high, demonstrating that the use of this processing route successfully activated the material, minimizing oxygen contamination and introducing efficiently crystalline defects in the microstructure of the compound. By doing so, no additional thermal processes as reported by other authors are necessary for hydrogen absorption.

All the samples reached similar hydrogen absorption capacities after 4 h, of 1.4 wt %.This shows that there is no significant difference in the hydrogen storage properties of the powder and the flakes parts produced. On the other hand, the increase in the number of passes (from 20 to 40) generated an improvement in the hydrogen absorption rate, which is possibly due to the increase of the surface area.

The cold-rolled TiFe investigated here showed a higher hydrogen absorption capacity than the TiFe produced by mechanical alloying, and the same hydrogen absorption capacity compared to the TiFe processed by mechanical grinding. This demonstrates that the CR process under inert atmosphere is an alternative route to produce TiFe compared to the high energy ball milling process: much simpler, with less time and energy consumption and better absorption properties.

Acknowledgments

The authors would like to thank FAPESP (grant number 2013/05987-8), CAPES and CNPq for the financial support.

REFERENCES

[1] Ouyang L, Cao Z, Wang H, Hu R, Zhu M. Application of dielectric barrier discharge plasma-assisted milling in energy storage materials – a review. J Alloy Comp 2017;691:422–35.
[2] Ouyang LZ, Cao ZJ, Wang H, Liu JW, Sun DL, Zhang QA, et al. Dual-tuning effect of in on the thermodynamic and kinetic properties of Mg_2Ni dehydrogenation. Int J Hydrogen Energy 2013;38:8881–7.
[3] Leng H, Yu Z, Yin J, Li Q, Wu Z, Chou K-C. Effects of Ce on the hydrogen storage properties of $TiFe_{0.9}Mn_{0.1}$ alloy. Int J Hydrogen Energy 2017;42:23731–6.
[4] Endo N, Suzuki S, Goshome K, Maeda T. Operation of a bench-scale TiFe-based alloy tank under mild conditions for low-cost stationary hydrogen storage. Int J Hydrogen Energy 2017;42:5246–51.
[5] Ali W, Hao Z, Li Z, Chen G, Wu Z, Lu X, et al. Effects of Cu and Y substitution on hydrogen storage performance of $TiFe_{0.86}Mn_{0.1}Y_{0.1-x}Cu_x$. Int J Hydrogen Energy 2017;42:16620–31.
[6] Lv P, Huot J. Hydrogen storage properties of $Ti_{0.95}FeZr_{0.05}$, $TiFe_{0.95}Zr_{0.05}$ and $TiFeZr_{0.05}$ alloys. Int J Hydrogen Energy 2016;41:22128–33.
[7] Reilly JJ, Wiswall RH. Formation and properties of iron titanium hydride. Inorg Chem 1974;13:218–22.
[8] Zaluski L, Tessier P, Ryan DH, Doner CB, Zaluska A, Stromolsen JO, et al. Amorphous and nanocrystalline Fe-Ti prepared by ball-milling. J Mater Res 1993;8:3059–68.
[9] Hotta H, Abe M, Kuji T, Uchida H. Synthesis of Ti–Fe alloys by mechanical alloying. J Alloy Comp 2007;439:221–6.
[10] Abe M, Kuji T. Hydrogen absorption of TiFe alloy synthesized by ball milling and post-annealing. J Alloy Comp 2007;446:200–3.
[11] Haraki T, Oishi K, Uchida H, Miyamoto Y, Abe M, Kokaji T, et al. Properties of hydrogen absorption by nano-structured FeTi alloys. Int J Mater Res 2008;99:507–12.
[12] Zadorozhnyy V, Klyamkin S, Zadorozhnyy M, Bermesheva O, Kaloshkin S. Hydrogen storage nanocrystalline TiFe intermetallic compound: synthesis by mechanical alloying and compacting. Int J Hydrogen Energy 2012;37:17131–6.
[13] Berdonosova EA, Klyamkin SN, Zadorozhnyy VY, Zadorozhnyy MY, Geodakian KV, Gorshenkov MV, et al. Calorimetric study of peculiar hydrogenation behavior of nanocrystalline TiFe. J Alloy Comp 2016;688:1181–5.
[14] Emami H, Edalati K, Matsuda J, Akiba E, Horita Z. Hydrogen storage performance of TiFe after processing by ball milling. Acta Mater 2015;88:190–5.
[15] Huot J. Nanocrystalline metal hydrides obtained by severe plastic deformations. Metals 2012;2:22–40.
[16] Edalati K, Matsuda J, Iwaoka H, Toh S, Akiba E, Horita Z. High-pressure torsion of TiFe intermetallics for activation of hydrogen storage at room temperature with heterogeneous nanostructure. Int J Hydrogen Energy 2013;38:4622–7.
[17] Edalati K, Matsuda J, Yanagida A, Akiba E, Horita Z. Activation of TiFe for hydrogen storage by plastic deformation using groove rolling and high-pressure torsion: similarities and differences. Int J Hydrogen Energy 2014;39:15589–94.
[18] Floriano R, Leiva DR, Carvalho JA, Ishikawa TT, Botta WJ. Cold rolling under inert atmosphere: a powerful tool for Mg activation. Int J Hydrogen Energy 2014;39:4959–65.
[19] Márquez JJ, Soyama J, de Araujo Silva R, Leiva DR, Floriano R, Ishikawa TT, et al. Processing of MgH_2 by extensive cold rolling under protective atmosphere. Int J Hydrogen Energy 2017;42:2201–8.
[20] Lü L, Lai MO. Mechanical alloying. US: Springer; 1998. p. 296.
[21] Ouyang LZ, Ye SY, Dong HW, Zhu M. Effect of interfacial free energy on hydriding reaction of Mg–Ni thin films. Appl Phys Lett 2007;90:021917–20.
[22] Suryanarayana C. Mechanical alloying and milling. Prog Mater Sci 2001;46:1–184.
[23] Abrashev B, Spassov T, Bliznakov S, Popov A. Microstructure and electrochemical hydriding/dehydriding properties of ball-milled TiFe-based alloys. Int J Hydrogen Energy 2010;35:6332–7.
[24] Ouyang L, Tang J, Zhao Y, Wang H, Yao X, Liu J, et al. Express penetration of hydrogen on Mg(10$\bar{1}$13) along the close-packed-planes. Sci Rep 2015;5:10776.
[25] Ouyang LZ, Yang XS, Zhu M, Liu JW, Dong HW, Sun DL, et al. Enhanced hydrogen storage kinetics and stability by synergistic effects of in situ formed $CeH_{2.73}$ and Ni in $CeH_{2.73}$-MgH_2-Ni nanocomposites. J Phys Colloid Chem 2014;118:7808–20.
[26] Schlapbach L, Seiler A, Stucki F. Surface segregation in FeTi and its catalytic effect on the hydrogenation. Mater Res Bull 1978;13:697–706.